

UDC 539.3

## ANALYSIS OF THE STRESS STATE FOR A LAYER WITH TWO INCUT CYLINDRICAL SUPPORTS

**Vitalii Yu. Miroshnikov**

[v.miroshnikov@khai.edu](mailto:v.miroshnikov@khai.edu)

ORCID: 0000-0002-9491-0181

**Oleksandr B. Savin**

[asavin344@gmail.com](mailto:asavin344@gmail.com)

ORCID: 0000-0002-2664-0255

**Mykhailo M. Hrebennikov**

[m.grebennikov@khai.edu](mailto:m.grebennikov@khai.edu)

ORCID: 0000-0001-7648-3027

**Vladyslav F. Demenko**

[v.demenko@khai.edu](mailto:v.demenko@khai.edu)

ORCID: 0000-0002-9555-4596

National Aerospace University

"Kharkiv Aviation Institute"

17, Chkalov str., Kharkov, 61070, Ukraine

*The stress state of a homogeneous isotropic layer under the action of a spatial static external load is studied. Two circular cylindrical supports are cut into the body of the layer parallel to its borders. The supports and body of the layer are rigidly coupled. The spatial problem theory of elasticity is solved using the analytical-numerical generalized Fourier method. The layer is considered in the Cartesian coordinate system, the supports are considered in the local cylindrical coordinates. Stresses are set on the upper and lower surfaces of the layer. The supports are considered as cylindrical cavities in a layer with zero displacements set on their surfaces. Satisfying the boundary conditions on the upper and lower surfaces of the layer, as well as on the cylindrical surfaces of the cavities, a system of infinite integro-algebraic equations, which are further reduced to linear algebraic ones, is obtained. An infinite system is solved by the reduction method. In the numerical studies, the parameters of integration oscillatory functions are analyzed, problems at different distances between supports are solved. A unit load in the form of a rapidly decreasing function is applied to the upper boundary between the supports. For these cases, an analysis of the stress state was performed on the surfaces of the layer between the supports and on the cylindrical surfaces in contact with the supports. The numerical analysis showed that when the distance between the supports increases, the stresses  $\sigma_x$  on the lower and upper surfaces of the layer and the stresses  $\tau_{pp}$  on the surfaces of the cavities increase. The use of the analytical-numerical method made it possible to obtain a result with an accuracy of  $10^{-4}$  for stress values from 0 to 1 at the order of the system of equations  $m=6$ . As the order of the system increases, the accuracy of fulfilling the boundary conditions will increase. The presented analytical-numerical solution can be used for high-precision determination of the stress-strain state of the presented problems type, as well a reference for problems based on numerical methods.*

**Keywords:** cylindrical cavities in a layer, generalized Fourier method, Lamé equation.

### Introduction

In mechanical engineering and the aerospace industry, it is needed to face the design of parts, which fastening to each other is cylindrical incut. The calculation of such details is usually done using methods of resistance of materials, construction mechanics or the finite elements method. That is, the calculation scheme is either simplified or an approximate method is used. But such methods are ineffective when it is necessary to have accurate values of the stress-strain state [1].

Analytical or analytical-numerical methods are used to increase the accuracy of calculation results. Thus, in papers [2–5], problems are solved for a layer with cavities perpendicular to its boundaries. But these methods cannot be used to solve problems of statics of spatial elastic bodies in the form of a layer with longitudinal cavities.

Furthermore, in case when cylindrical cavities are parallel to the layer boundaries, stationary problems of diffraction of elastic waves, where the Fourier method is used in combination with the method of images, are considered in papers [6–9]. But this approach does not allow to solve problems with more than three boundary surfaces.

For spatial models with a large number of boundary surfaces and high accuracy of the stress state determination, the analytical-numerical generalized Fourier method is the most effective [10]. Based on this method, the problems for a cylinder with cylindrical cavities or inclusions [11–14], for a half-space with a cavity [15], for a layer with one cavity [16, 17], a layer with several cylindrical cavities [18], a layer with one [19] or with two inclusions [20] are considered. In the listed papers, the problems, boundary conditions and algorithms for the solution of which do not allow applying them to problems for a layer with cylindrical incut supports, are considered.

This work is licensed under a Creative Commons Attribution 4.0 International License.

© Vitalii Yu. Miroshnikov, Oleksandr B. Savin, Mykhailo M. Hrebennikov, Vladyslav F. Demenko, 2023

The papers [21, 22], which solve problems for a layer with one cylindrical cavity [21] and for a layer with a cylindrical pipe [22], are most relevant to the topic under consideration. The boundary conditions in these papers allow to consider the proposed model as a layer with one incut support. But additional conditions are required to take into account the second support.

Given the absence of a method for calculating problems for a layer with incut cylindrical supports in the presence of similar calculation schemes in practice, the chosen topic is relevant and needs to be studied.

For a high-precision solution of the problem, the analytical-numerical generalized Fourier method will be used in the paper.

**Problem statement**

The elastic homogeneous layer has two cylindrical cavities that are located parallel to its boundaries. Cavity radii are  $R_p$ , where  $p$  – cavity number.

Cavities will be considered in local cylindrical coordinate systems  $(\rho_p, \varphi_p, z)$ , layer – in the Cartesian coordinate system  $(x, y, z)$ . Layer boundaries are located at a distance  $y=h$  and  $y=-\tilde{h}$  (Fig. 1).

It is necessary to find the solution of the Lamé equation, provided that at the upper boundary of the layer stresses

$F\vec{U}(x, z)|_{y=h} = \vec{F}_h^0(x, z)$  are given, and on the bottom one – stresses  $F\vec{U}(x, z)|_{y=-\tilde{h}} = \vec{F}_{\tilde{h}}^0(x, z)$ , on the cavity surfaces – displacements  $\vec{U}(\varphi_p, z)|_{\rho_p=R_p} = \vec{U}_p^0(\varphi_p, z)$ , where  $\vec{U}$  – displacement in a layer;

$$F\vec{U} = 2 \cdot G \cdot \left[ \frac{\sigma}{1-2 \cdot \sigma} \vec{n} \cdot \text{div} \vec{U} + \frac{\partial}{\partial n} \vec{U} + \frac{1}{2} (\vec{n} \times \text{rot} \vec{U}) \right] - \text{stress operator};$$

$$\vec{F}_h^0(x, z) = \tau_{yx}^{(h)} \vec{e}_x + \sigma_y^{(h)} \vec{e}_y + \tau_{yz}^{(h)} \vec{e}_z;$$

$$\vec{F}_{\tilde{h}}^0(x, z) = \tau_{yx}^{(\tilde{h})} \vec{e}_x + \sigma_y^{(\tilde{h})} \vec{e}_y + \tau_{yz}^{(\tilde{h})} \vec{e}_z; \tag{1}$$

$$\vec{U}_p^0(\varphi_p, z) = U_\rho^{(p)} \vec{e}_\rho + U_\varphi^{(p)} \vec{e}_\varphi + U_z^{(p)} \vec{e}_z,$$

known functions, which will be considered rapidly decreasing from the origin of the coordinates along the axis  $z$  and  $x$ .

**Solution method**

The basic solutions of the Lamé equation for Cartesian and cylindrical coordinate systems are chosen in the form [10]:

$$\begin{aligned} \vec{u}_k^\pm(x, y, z; \lambda, \mu) &= N_k^{(d)} e^{i(\lambda z + \mu x) \pm \gamma y}; \\ \vec{R}_{k,m}(\rho, \varphi, z; \lambda) &= N_k^{(p)} I_m(\lambda \rho) e^{i(\lambda z + m\varphi)}; \end{aligned} \tag{2}$$

$$\vec{S}_{k,m}(\rho, \varphi, z; \lambda) = N_k^{(p)} \left[ (\text{sign } \lambda)^m K_m(|\lambda| \rho) \cdot e^{i(\lambda z + m\varphi)} \right]; k = 1, 2, 3;$$

$$N_1^{(d)} = \frac{1}{\lambda} \nabla; N_2^{(d)} = \frac{4}{\lambda} (\sigma - 1) \vec{e}_2^{(1)} + \frac{1}{\lambda} \nabla(y \cdot); N_3^{(d)} = \frac{i}{\lambda} \text{rot}(\vec{e}_3^{(1)} \cdot); N_1^{(p)} = \frac{1}{\lambda} \nabla;$$

$$N_2^{(p)} = \frac{1}{\lambda} \left[ \nabla \left( \rho \frac{\partial}{\partial \rho} \right) + 4(\sigma - 1) \left( \nabla - \vec{e}_3^{(2)} \frac{\partial}{\partial z} \right) \right]; N_3^{(p)} = \frac{i}{\lambda} \text{rot}(\vec{e}_3^{(2)} \cdot); \gamma = \sqrt{\lambda^2 + \mu^2}, -\infty < \lambda, \mu < \infty,$$

where  $I_m(x)$ ,  $K_m(x)$  – modified Bessel functions;  $\vec{R}_{k,m}$ ,  $\vec{S}_{k,m}$  – inner and outer solutions of the Lamé equation for the cylinder, respectively;  $\vec{u}_k^{(-)}$ ,  $\vec{u}_k^{(+)}$  – solutions of the Lamé equation for a layer;  $\sigma$  – Poisson's ratio.

The problem solution is given in the form [18]

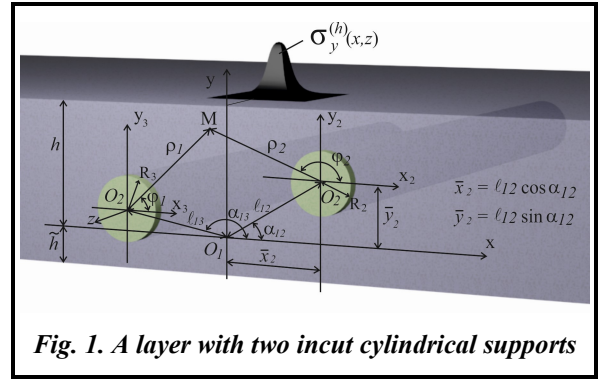


Fig. 1. A layer with two incut cylindrical supports

$$\begin{aligned} \bar{U}_0 = & \sum_{p=1}^2 \sum_{k=1}^3 \int_{-\infty}^{\infty} \sum_{m=-\infty}^{\infty} B_{k,m}^{(p)}(\lambda) \cdot \bar{S}_{k,m}(\rho_p, \varphi_p, z; \lambda) d\lambda + \\ & + \sum_{k=1}^3 \int_{-\infty}^{\infty} \int_{-\infty}^{\infty} (H_k(\lambda, \mu) \cdot \bar{u}_k^{(+)}(x, y, z; \lambda, \mu) + \tilde{H}_k(\lambda, \mu) \cdot \bar{u}_k^{(-)}(x, y, z; \lambda, \mu)) d\mu d\lambda, \end{aligned} \quad (3)$$

where  $\bar{S}_{k,m}(\rho_p, \varphi_p, z; \lambda)$ ,  $\bar{R}_{k,m}(\rho_p, \varphi_p, z; \lambda)$ ,  $\bar{u}_k^{(+)}(x, y, z; \lambda, \mu)$  and  $\bar{u}_k^{(-)}(x, y, z; \lambda, \mu)$  – basic solutions given by formulas (2), and unknown functions  $H_k(\lambda, \mu)$ ,  $\tilde{H}_k(\lambda, \mu)$ ,  $B_{k,m}^{(p)}(\lambda)$  must be found from the boundary conditions (1).

The formulas [10] are used for transition between coordinate systems:

– for transition from solutions  $\bar{S}_{k,m}$  of cylindrical coordinate system to layer solutions  $\bar{u}_k^{(-)}$  (at  $y>0$ ) and  $\bar{u}_k^{(+)}$  (at  $y<0$ )

$$\begin{aligned} \bar{S}_{k,m}(\rho_p, \varphi_p, z; \lambda) = & \frac{(-i)^m}{2} \int_{-\infty}^{\infty} \omega_{\mp}^m \cdot e^{-i\mu\bar{x}_p \pm \gamma\bar{y}_p} \cdot \bar{u}_k^{(\mp)} \cdot \frac{d\mu}{\gamma}, \quad k = 1, 3; \\ \bar{S}_{2,m}(\rho_p, \varphi_p, z; \lambda) = & \frac{(-i)^m}{2} \int_{-\infty}^{\infty} \omega_{\mp}^m \cdot \left( \left( \pm m \cdot \mu - \frac{\lambda^2}{\gamma} \pm \lambda^2 \bar{y}_p \right) \bar{u}_1^{(\mp)} \mp \lambda^2 \bar{u}_2^{(\mp)} \pm \pm 4\mu(1-\sigma) \bar{u}_3^{(\mp)} \right) \cdot \frac{e^{-i\mu\bar{x}_p \pm \gamma\bar{y}_p} d\mu}{\gamma^2}, \end{aligned} \quad (4)$$

where  $\gamma = \sqrt{\lambda^2 + \mu^2}$ ,  $\omega_{\mp}(\lambda, \mu) = \frac{\mu \mp \gamma}{\lambda}$ ,  $m = 0, \pm 1, \pm 2, \dots$ ;

– for transition from the layer solutions  $\bar{u}_k^{(+)}$  and  $\bar{u}_k^{(-)}$  to cylindrical coordinate system solutions  $\bar{R}_{k,m}$

$$\begin{aligned} \bar{u}_k^{(\pm)}(x, y, z) = & e^{i\mu\bar{x}_p \pm \gamma\bar{y}_p} \cdot \sum_{m=-\infty}^{\infty} (i \cdot \omega_{\mp})^m \bar{R}_{k,m}, \quad (k = 1, 3); \\ \bar{u}_2^{(\pm)}(x, y, z) = & e^{i\mu\bar{x}_p \pm \gamma\bar{y}_p} \cdot \sum_{m=-\infty}^{\infty} \left[ (i \cdot \omega_{\mp})^m \cdot \lambda^{-2} \left( (m \cdot \mu + \bar{y}_p \cdot \lambda^2) \cdot \bar{R}_{1,m} \pm \gamma \cdot \bar{R}_{2,m} + 4\mu(1-\sigma) \bar{R}_{3,m} \right) \right], \end{aligned} \quad (5)$$

where  $\bar{R}_{k,m} = \tilde{b}_{k,m}(\rho_p, \lambda) \cdot e^{i(m\varphi_p + \lambda z)}$ ;  $\tilde{b}_{1,n}(\rho, \lambda) = \bar{e}_{\rho} \cdot I'_n(\lambda\rho) + i \cdot I_n(\lambda\rho) \cdot \left( \bar{e}_{\varphi} \frac{n}{\lambda\rho} + \bar{e}_z \right)$ ;

$\tilde{b}_{2,n}(\rho, \lambda) = \bar{e}_{\rho} \cdot [(4\sigma - 3) \cdot I'_n(\lambda\rho) + \lambda\rho I''_n(\lambda\rho)] + \bar{e}_{\varphi} i \cdot m \left( I'_n(\lambda\rho) + \frac{4(\sigma - 1)}{\lambda\rho} I_n(\lambda\rho) \right) + \bar{e}_z i \lambda \rho I'_n(\lambda\rho)$ ;

$\tilde{b}_{3,n}(\rho, \lambda) = - \left[ \bar{e}_{\rho} \cdot I_n(\lambda\rho) \frac{n}{\lambda\rho} + \bar{e}_{\varphi} \cdot i \cdot I'_n(\lambda\rho) \right]$ ;  $\bar{e}_{\rho}$ ,  $\bar{e}_{\varphi}$ ,  $\bar{e}_z$  are unit vectors in the cylindrical coordinate system;

– for transition from the solutions of the cylinder with the number  $p$  to the solutions of the cylinder with the number  $q$

$$\begin{aligned} \bar{S}_{k,m}(\rho_p, \varphi_p, z; \lambda) = & \sum_{n=-\infty}^{\infty} \bar{b}_{k,pq}^{mn}(\rho_q) \cdot e^{i(n\varphi_q + \lambda z)}, \quad k = 1, 2, 3; \\ \bar{b}_{1,pq}^{mn}(\rho_q) = & (-1)^n \tilde{K}_{m-n}(\lambda \ell_{pq}) \cdot e^{i(m-n)\alpha_{pq}} \cdot \tilde{b}_{1,n}(\rho_q, \lambda), \\ \bar{b}_{3,pq}^{mn}(\rho_q) = & (-1)^n \tilde{K}_{m-n}(\lambda \ell_{pq}) \cdot e^{i(m-n)\alpha_{pq}} \cdot \tilde{b}_{3,n}(\rho_q, \lambda); \\ \bar{b}_{2,pq}^{mn}(\rho_q) = & (-1)^n \left\{ \tilde{K}_{m-n}(\lambda \ell_{pq}) \cdot \tilde{b}_{2,n}(\rho_q, \lambda) - \frac{\lambda}{2} \ell_{pq} \cdot \left[ \tilde{K}_{m-n+1}(\lambda \ell_{pq}) + \tilde{K}_{m-n-1}(\lambda \ell_{pq}) \right] \cdot \tilde{b}_{1,n}(\rho_q, \lambda) \right\} \cdot e^{i(m-n)\alpha_{pq}}, \end{aligned} \quad (6)$$

where  $\alpha_{pq}$  is the angle between the axis  $x_p$  and segment  $\ell_{pq}$ ,  $\tilde{K}_m(x) = (\text{sign}(x))^m \cdot K_m(|x|)$ .

To meet the boundary conditions on the upper and lower boundaries of the layer, we find the stress for the right part of vector (3). We equate the obtained vector at  $y=h$  given as  $\bar{F}_h^0(x, z)$ , and at  $y=-\tilde{h}$  given as

$\vec{F}_h^0(x, z)$ , represented by the double Fourier integral. Basic solutions  $\vec{S}_{k,m}(\rho_p, \varphi_p, z; \lambda)$ , with the help of the transition formulas (4), will be rewritten in the Cartesian coordinate system through basic solutions  $\vec{u}_k^{(-)}(x, y, z; \lambda, \mu)$  at  $y=h$  and  $\vec{u}_k^{(+)}(x, y, z; \lambda, \mu)$  at  $y=-\tilde{h}$ . In this way, we get three equations for the upper boundary of the layer (one for each projection) and three equations for the lower boundary of the layer with 12 unknowns  $H_k(\lambda, \mu)$ ,  $\tilde{H}_k(\lambda, \mu)$ ,  $B_{k,m}^{(2)}(\lambda)$ ,  $B_{k,m}^{(3)}(\lambda)$ .

From this system of equations, we find  $H_k(\lambda, \mu)$  and  $\tilde{H}_k(\lambda, \mu)$  by  $B_{k,m}^{(p)}(\lambda)$ .

To satisfy the boundary conditions on the surface of each cavity  $p$ , the right-hand part of (3) will be rewritten using the transition formulas (5) and (6) in the local cylindrical coordinate system of each cavity  $p$  through basic solutions  $\vec{R}_{k,m}, \vec{S}_{k,m}$ . The resulting vector, at  $\rho_p=R_p$ , equals to the given as  $\vec{U}_p^0(\varphi_p, z)$ , represented by the double Fourier integral. As a result, for each cylinder with the number  $p$ , we will get three infinite systems of linear algebraic equations with respect to  $B_{k,m}^{(p)}(\lambda)$ , which contain  $H_k(\lambda, \mu)$  and  $\tilde{H}_k(\lambda, \mu)$ .

In this way, we will get 12 integro-algebraic equations with 12 unknowns  $H_k(\lambda, \mu)$ ,  $\tilde{H}_k(\lambda, \mu)$ ,  $B_{k,m}^{(p)}(\lambda)$ . Excluding the previously found from these equations  $H_k(\lambda, \mu)$  and  $\tilde{H}_k(\lambda, \mu)$  by  $B_{k,m}^{(p)}(\lambda)$  and getting rid of series over  $m$  and integrals over  $\lambda$ , we will get 12 infinite linear algebraic equations of the second kind to determine the unknowns  $B_{k,m}^{(p)}(\lambda)$ .

We will apply the reduction method to the obtained infinite systems of equations, as a result of which we will find the coefficients  $B_{k,m}^{(p)}(\lambda)$ . Now  $B_{k,m}^{(p)}(\lambda)$  will be substituted in the expression for  $H_k(\lambda, \mu)$  and  $\tilde{H}_k(\lambda, \mu)$ . Thus, all unknowns of expression (3) will be found.

The numerical solutions of the infinite system presented in the paper by the reduction method showed its convergence, which satisfies the boundary conditions with high accuracy.

**Numerical studies of the stressed state**

There are two cylindrical cavities in the elastic isotropic layer (Fig. 1). Poisson's ratio of the layer (ABS plastic) is  $\sigma_0=0.38$ , modulus of elasticity is  $E_0=1700 \text{ N/mm}^2$ . Geometric parameters of the model are:  $R_2=R_3=5 \text{ mm}$ ,  $h=12 \text{ mm}$ ,  $\tilde{h}=12 \text{ mm}$ ,  $\alpha_{12}=0$ ,  $\alpha_{13}=\pi$ . We will set the distance to the cavities in two versions  $L_{12}=L_{13}=15 \text{ mm}$  and  $L_{12}=L_{13}=30 \text{ mm}$ .

Normal stresses in the form of a unit wave  $\sigma_y^{(h)}(x, z) = -10^8 \cdot (z^2 + 10^2)^{-2} \cdot (x^2 + 10^2)^{-2}$ , and zero tangential stresses  $\tau_{yx}^{(h)} = \tau_{yz}^{(h)} = 0$  are set at the upper boundary of the layer, stresses  $\sigma_y^{(\tilde{h})}(x, z) = \tau_{yx}^{(\tilde{h})}(x, z) = \tau_{yz}^{(\tilde{h})}(x, z) = 0$  are given at the lower boundary of the layer.

The infinite system was truncated by the parameter  $m=6$  (the number of terms of the Fourier series and the order of the system of equations).

The integrals were calculated using Philo's quadrature formulas. The accuracy of meeting the boundary conditions with the specified  $m$  and the specified geometric parameters is not less than  $10^{-4}$  at values from 0 to 1. This corresponds to paper [16], where a detailed analysis of the convergence of the equations with respect to different values of  $m$  for a layer with cavities was carried out.

Fig. 2 shows the schedule of specified stresses  $\sigma_y$  and their corresponding stresses  $\sigma_x$  on the upper and lower surfaces of the layer at  $z=0$ .

When increasing the distance between supports, stresses  $\sigma_x$  grow on the upper and lower surfaces of the layer. At  $L_{12}=L_{13}=30 \text{ mm}$  maximum stresses  $\sigma_x$  on the upper

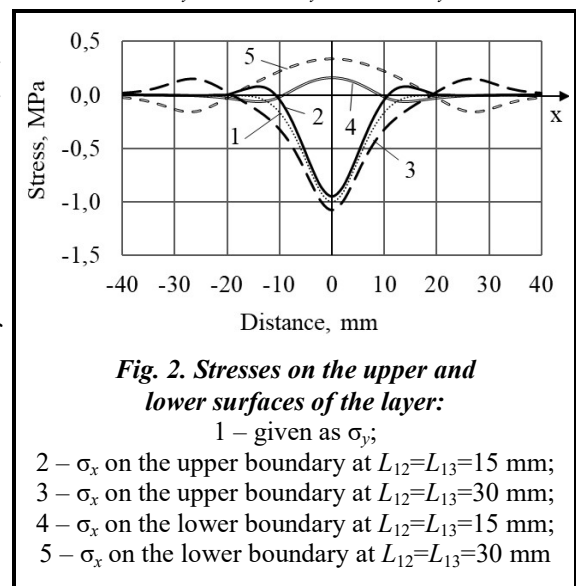


**Fig. 2. Stresses on the upper and lower surfaces of the layer:**

1 – given as  $\sigma_y$ ;

2 –  $\sigma_x$  on the upper boundary at  $L_{12}=L_{13}=15 \text{ mm}$ ;

3 –  $\sigma_x$  on the upper boundary at  $L_{12}=L_{13}=30 \text{ mm}$ ;

4 –  $\sigma_x$  on the lower boundary at  $L_{12}=L_{13}=15 \text{ mm}$ ;

5 –  $\sigma_x$  on the lower boundary at  $L_{12}=L_{13}=30 \text{ mm}$

surface of the layer exceed the specified values (Fig. 2, line 3). Also, at  $L_{12}=L_{13}=30$  mm, a significant increase in stresses  $\sigma_x$  is observed on the upper and lower surfaces of the layer near the supports.

Fig. 3 shows stresses  $\sigma_p$  on the support surface located on the right ( $p=2$ ) at  $z=0$ .

When the distance between the supports increases, the maximum stresses  $\sigma_p$  on the surfaces of the cylinders decrease (Fig. 3), shifting to the horizontal axis in the direction of the load.

Stresses  $\sigma_p$  graphs on the surface of the support located on the left ( $p=3$ ), are symmetrical to Fig. 3 relative to the vertical axis ( $\pi/2$ ).

Stresses  $\sigma_\varphi$  and  $\sigma_z$  graphs almost coincide with each other and have the same appearance as stresses  $\sigma_p$ , only with smaller values. So stresses  $\sigma_{\varphi, \max}=-0.08794$  MPa (at  $\varphi=2.74889$ ,  $L_{12}=L_{13}=30$  mm),  $\sigma_{\varphi, \max}=-0.26128$  MPa (at  $\varphi=2.356$ ,  $L_{12}=L_{13}=15$  mm),  $\sigma_{z, \max}=-0,0886$  MPa (at  $\varphi=2.74889$ ,  $L_{12}=L_{13}=30$  mm),  $\sigma_{\varphi, \max}=-0,26548$  MPa (at  $\varphi=2.356$ ,  $L_{12}=L_{13}=15$  mm).

Fig. 4 shows stresses  $\tau_{p\varphi}$  on the support surface located on the right ( $p=2$ ) at  $z=0$ .

When increasing the distance between supports, stresses  $\tau_{p\varphi}$  on the surfaces of the cylinders increase (Fig. 4).

Stresses graphs  $\tau_{p\varphi}$  on the surface of the support located on the left ( $p=3$ ), are symmetrical to Fig. 4 with respect to the vertical axis ( $\pi/2$ ) and with a different sign.

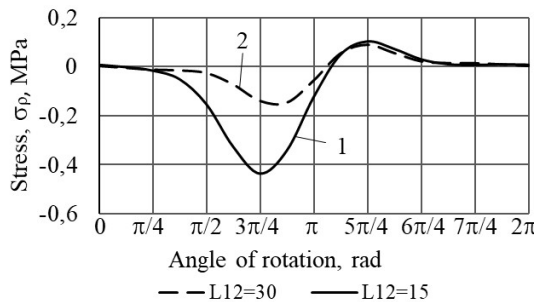


Fig. 3. Stresses  $\sigma_p$  on the cavity surface  $p=2$

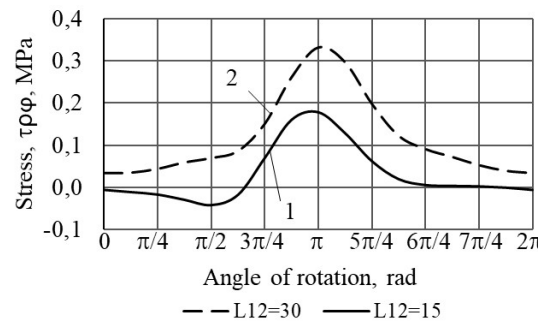


Fig. 4. Stresses  $\tau_{p\varphi}$  on the cavity surface  $p=2$

## Conclusions

An analytical-numerical method for solving the spatial problem of the theory of elasticity for a layer rigidly connected to two circular cylindrical supports cut into it is proposed. The problem is reduced to an infinite system of linear algebraic equations, which allows the reduction method to be applied to it. Numerical studies give reasons to claim that its solution can be found with any accuracy by the proposed method, which is confirmed by the high accuracy of the fulfillment of the boundary conditions.

The presented comparative analysis shows that in the given model the stresses  $\sigma_x$  increase as the distance between the supports increases on the lower and upper surfaces of the layer, as well as stresses  $\tau_{p\varphi}$  on cavity surfaces.

The suggested solution method allows to obtain the stress-strain state for a layer with only two longitudinal circular cylindrical supports. For further development of this method, the number of supports can be increased and cylindrical inhomogeneities between the supports can be added.

## References

1. Azarov, A. D., Zhuravlev, G. A., & Piskunov, A. S. (2015). *Sravnitelnyy analiz analiticheskogo i chislennogo metodov resheniya ploskoy zadachi o kontakte uprugikh tsilindrov* [Comparative analysis of analytical and numerical methods for solving the plane problem of elastic cylinder contact]. *Innovatsionnaya nauka – Innovative Science*, no. 1–5, pp. 5–13 (in Russian).
2. Guz, A. N., Kosmodamianskiy, A. S., Shevchenko, V. P., Nemish, Yu. N., & Avdyushina, Ye. V. (1998). *Mekhanika kompozitov* [Mechanics of composites]: in 12 vols. Vol. 7. *Kontsentratsiya napryazheniy* [Stress concentration]. Kyiv: Naukova dumka, 387 p. (in Russian).
3. Vaysfel'd, N., Popov, G., & Reut, V. (2015). The axisymmetric contact interaction of an infinite elastic plate with an absolutely rigid inclusion. *Acta Mechanica*, vol. 226, iss. 3, pp. 797–810. <https://doi.org/10.1007/s00707-014-1229-7>.

4. Popov, G. Y. & Vaisfel'd, N. D. (2014). Solving an axisymmetric problem of elasticity for an infinite plate with a cylindrical inclusion with allowance for its specific weight. *International Applied Mechanics*, vol. 50, iss. 6, pp. 627–636. <https://doi.org/10.1007/s10778-014-0661-7>.
5. Bobyleva, T. (2016). Approximate method of calculating stresses in layered array. *Procedia Engineering*, vol. 153, pp. 103–106. <https://doi.org/10.1016/j.proeng.2016.08.087>.
6. Guz, A. N., Kubenko, V. D., & Cherevko, M. A. (1978). *Difraktsiya uprugikh voln* [Diffraction of elastic waves]. Kyiv: Naukova dumka, 307 p. (in Russian).
7. Grinchenko, V. T. & Meleshko, V. V. (1981). *Garmonicheskiye kolebaniya i volny v uprugikh telakh* [Harmonic oscillations and waves in elastic bodies]. Kyiv: Naukova dumka, 284 p. (in Russian).
8. Volchkov, V. V., Vukolov, D. S., & Storozhev, V. I. (2016). *Difraktsiya voln sdviga na vnutrennikh tunnel'nykh tsilindricheskikh neodnorodnostyakh v vide polosti i vklyucheniya v uprugom sloye so svobodnymi granyami* [Diffraction of shear waves on internal tunnel cylindrical inhomogeneities in the form of a cavity and inclusion in the elastic layer with free face]. *Mekhanika tverdogo tela – Mechanics of Rigid Bodies*, iss. 46, pp. 119–133 (in Russian).
9. Grinchenko, V. T. & Ulitko, A. F. (1968). An exact solution of the problem of stress distribution close to a circular hole in an elastic layer. *Soviet Applied Mechanics*, vol. 4, iss. 10, pp. 31–37. <https://doi.org/10.1007/BF00886618>.
10. Nikolayev, A. G. & Protsenko, V. S. (2011). *Obobshchennyi metod Furye v prostranstvennykh zadachakh teorii uprugosti* [The generalized Fourier method in spatial problems of the theory of elasticity]. Kharkiv: National Aerospace University «Kharkiv Aviation Institute», 344 p. (in Russian).
11. Nikolaev, A. G. & Tanchik, E. A. (2015). The first boundary-value problem of the elasticity theory for a cylinder with  $N$  cylindrical cavities. *Numerical Analysis and Applications*, vol. 8, iss. 2, pp. 148–158. <https://doi.org/10.1134/S1995423915020068>.
12. Nikolaev, A. G. & Tanchik, E. A. (2016). Stresses in an infinite circular cylinder with four cylindrical cavities. *Journal of Mathematical Sciences*, vol. 217, iss. 3, pp. 299–311. <https://doi.org/10.1007/s10958-016-2974-z>.
13. Nikolaev, A. G. & Tanchik, E. A. (2016). Model of the stress state of a unidirectional composite with cylindrical fibers forming a tetragonal structure. *Mechanics of Composite Materials*, vol. 52, iss. 2, pp. 177–188. <https://doi.org/10.1007/s11029-016-9571-6>.
14. Nikolaev, A. G. & Tanchik, E. A. (2016). Stresses in an elastic cylinder with cylindrical cavities forming a hexagonal structure. *Journal of Applied Mechanics and Technical Physics*, vol. 57, iss. 6, pp. 1141–1149. <https://doi.org/10.1134/S0021894416060237>.
15. Nikolayev, A. G. & Orlov, Ye. M. (2012). *Resheniye pervoy osesimmetrichnoy termouprugoy krayevoy zadachi dlya transversalno-izotropnogo poluprostranstva so sferoidalnoy polostyu* [Solution of the first axisymmetric thermoelastic boundary value problem for a transversally isotropic half-space with a spheroidal cavity]. *Problemy vychislitel'noy mekhaniki i prochnosti konstruksiy – Problems of computational mechanics and strength of structures*, iss. 20, pp. 253–259 (in Russian).
16. Miroshnikov, V. Yu. (2020). Stress state of an elastic layer with a cylindrical cavity on a rigid foundation. *International Applied Mechanics*, vol. 56, iss. 3, pp. 372–381. <https://doi.org/10.1007/s10778-020-01021-x>.
17. Miroshnikov, V., Denysova, T., & Protsenko, V. (2019). *Doslidzhennia pershoi osnovnoi zadachi teorii pruzhnosti dlia sharu z tsylindrychnoiu porozhnyoiu* [The study of the first main problem of the theory of elasticity for a layer with a cylindrical cavity]. *Opir materialiv i teoriia sporud – Strength of Materials and Theory of Structures*, no. 103, pp. 208–218 (in Ukrainian). <https://doi.org/10.32347/2410-2547.2019.103.208-218>.
18. Miroshnikov, V. Yu. & Protsenko, V. S. (2019). Determining the stress state of a layer on a rigid base weakened by several longitudinal cylindrical cavities. *Journal of Advanced Research in Technical Science*, iss. 17, pp. 11–21. <https://doi.org/10.26160/2474-5901-2019-17-11-21>.
19. Miroshnikov, V. Yu., Medvedeva, A. V., & Oleshkevich, S. V. (2019). Determination of the stress state of the layer with a cylindrical elastic inclusion. *Materials Science Forum*, vol. 968, pp. 413–420. <https://doi.org/10.4028/www.scientific.net/MSF.968.413>.
20. Miroshnikov, V. Yu., Savin, O. B., Hrebennikov, M. M., & Pohrebniak, O. A. (2022). Analysis of the stress state of a layer with two cylindrical elastic inclusions and mixed boundary conditions. *Journal of Mechanical Engineering – Problemy mashynobuduvannia*, vol. 25, no. 2, pp. 22–29. <https://doi.org/10.15407/pmach2022.02.022>.
21. Hrebennikov, M. M. & Myronov, K. V. (2021). *Analiz napruzhenoho stanu sharu z pozdovzhnoiu porozhnyoiu ta zadanyimi nevlasno mishanymi hranychnymi umovamy* [Analysis of the stress state of a layer with a longitudinal cavity and given improperly mixed boundary conditions]. *Science, theory and practice: Abstracts of XXIX International Scientific and Practical Conference, Japan, Tokyo*, pp. 536–540 (in Ukrainian).
22. Miroshnikov, V. (2023). Rotation of the layer with the cylindrical pipe around the rigid cylinder. In: *Advances in Mechanical and Power Engineering. CAMPE 2021. Lecture Notes in Mechanical Engineering*. Cham: Springer, pp. 314–322. [https://doi.org/10.1007/978-3-031-18487-1\\_32](https://doi.org/10.1007/978-3-031-18487-1_32).

Received 23 February 2023

## Аналіз напруженого стану шару з двома циліндричними врізаними опорами

В. Ю. Мірошніков, О. Б. Савін, М. М. Гребенніков, В. Ф. Деменко

Національний аерокосмічний університет ім. М. Є. Жуковського «Харківський авіаційний інститут»,  
61070, Україна, Харків, вул. Чкалова, 17

Досліджується напружений стан однорідного ізотропного шару при дії просторового статичного зовнішнього навантаження. Дві кругові циліндричні опори врізані в тіло шару паралельно його межах. Опори та тіло шару жорстко спряжені між собою. Просторова задача теорії пружності розв'язується за допомогою аналітико-чисельного узагальненого методу Фур'є. Шар розглядається в декартовій системі координат, опори – у локальних циліндричних. На верхній та нижній поверхнях шару задані напруження. Опори розглядаються у вигляді циліндричних порожнин у шарі із заданими на їх поверхнях нульовими переміщеннями. Задовольняючи граничним умовам на верхній і нижній поверхнях шару, а також на циліндричних поверхнях порожнин, отримано системи нескінченних інтегро-алгебраїчних рівнянь, які в подальшому зведені до лінійних алгебраїчних. Нескінченна система розв'язується методом редуції. У чисельних дослідженнях проаналізовано параметри інтегрування коливних функцій, розв'язані задачі при різних відстанях між опорами. Одиничне навантаження у вигляді швидко спадаючої функції прикладено на верхній межі між опорами. Для цих випадків проведено аналіз напруженого стану на поверхнях шару між опорами та на циліндричних поверхнях, що контактують з опорами. Чисельний аналіз показав, що при збільшенні відстані між опорами зростають напруження  $\sigma_x$  на нижній та верхній поверхнях шару й напруження  $\tau_{\rho\rho}$  на поверхнях порожнин. Використання аналітико-чисельного методу дало можливість отримати результат із точністю  $10^{-4}$  для значень напружень від 0 до 1 при порядку системи рівнянь  $m=6$ . При збільшенні порядку системи точність виконання граничних умов зростатиме. Представлене аналітико-чисельне розв'язання може використовуватися для високоточного визначення напружено-деформованого стану представленої типу задач, а також як еталонне для задач, що базуються на чисельних методах.

**Ключові слова:** циліндричні порожнини в шарі, узагальнений метод Фур'є, рівняння Ламе.

## Література

1. Азаров А. Д., Журавлев Г. А., Пискунов А. С. Сравнительный анализ аналитического и численного методов решения плоской задачи о контакте упругих цилиндров. *Инновационная наука*. 2015. № 1–2. С. 5–13.
2. Гузь А. Н., Космодамианский А. С., Шевченко В. П., Немиш Ю. Н., Авдюшина Е. В. Механика композитов: в 12 т. Т. 7. Концентрация напряжений. Киев: Наукова думка, 1998. 387 с.
3. Vaysfel'd N., Popov G., Reut V. The axisymmetric contact interaction of an infinite elastic plate with an absolutely rigid inclusion. *Acta Mechanica*. 2015. Vol. 226. Iss. 3. P. 797–810. <https://doi.org/10.1007/s00707-014-1229-7>.
4. Попов Г. Я., Вайсфельд Н. Д. Осесимметричная задача теории упругости для бесконечной плиты с цилиндрическим включением при учете ее удельного веса. *Прикладная механика*. 2014. Т. 50. № 6. С. 27–38.
5. Bobyleva T. Approximate method of calculating stresses in layered array. *Procedia Engineering*. 2016. Vol. 153. P. 103–106. <https://doi.org/10.1016/j.proeng.2016.08.087>.
6. Гузь А. Н., Кубенко В. Д., Черевко М. А. Дифракция упругих волн. Киев: Наукова думка, 1978. 307 с.
7. Гринченко В. Т., Мелешко В. В. Гармонические колебания и волны в упругих телах. Киев: Наукова думка, 1981. 284 с.
8. Волчков В. В., Вуколов Д. С., Сторожев В. И. Дифракция волн сдвига на внутренних туннельных цилиндрических неоднородностях в виде полости и включения в упругом слое со свободными гранями. *Механика твердого тела*. 2016. Вып. 46. С. 119–133.
9. Grinchenko V. T., Ulitko A. F. An exact solution of the problem of stress distribution close to a circular hole in an elastic layer. *Soviet Applied Mechanics*. 1968. Vol. 4. Iss. 10. P. 31–37. <https://doi.org/10.1007/BF00886618>.
10. Николаев А. Г., Проценко В. С. Обобщенный метод Фурье в пространственных задачах теории упругости. Харьков: Национальный аэрокосмический университет им. Н. Е. Жуковского «Харьковский авиационный институт», 2011. 344 с.
11. Nikolaev A. G., Tanchik E. A. The first boundary-value problem of the elasticity theory for a cylinder with N cylindrical cavities. *Numerical Analysis and Applications*. 2015. Vol. 8. Iss. 2. P. 148–158. <https://doi.org/10.1134/S1995423915020068>.
12. Nikolaev A. G., Tanchik E. A. Stresses in an infinite circular cylinder with four cylindrical cavities. *Journal of Mathematical Sciences*. 2016. Vol. 217. Iss. 3. P. 299–311. <https://doi.org/10.1007/s10958-016-2974-z>.
13. Nikolaev A. G., Tanchik E. A. Model of the stress state of a unidirectional composite with cylindrical fibers forming a tetragonal structure. *Mechanics of Composite Materials*. 2016. Vol. 52. Iss. 2. P. 177–188. <https://doi.org/10.1007/s11029-016-9571-6>.

14. Nikolaev A. G., Tanchik E. A. Stresses in an elastic cylinder with cylindrical cavities forming a hexagonal structure. *Journal of Applied Mechanics and Technical Physics*. 2016. Vol. 57. Iss. 6. P. 1141–1149. <https://doi.org/10.1134/S0021894416060237>.
15. Николаев А. Г., Орлов Е. М. Решение первой осесимметричной термоупругой краевой задачи для трансверсально-изотропного полупространства со сфероидальной полостью. *Проблемы вычислительной механики и прочности конструкций*. 2012. Вып. 20. С. 253–259.
16. Miroshnikov V. Yu. Stress state of an elastic layer with a cylindrical cavity on a rigid foundation. *International Applied Mechanics*. 2020. Vol. 56. Iss. 3. P. 372–381. <https://doi.org/10.1007/s10778-020-01021-x>.
17. Мірошніков В. Ю., Денисова Т. В., Проценко В. С. Дослідження першої основної задачі теорії пружності для шару з циліндричною порожниною. *Опір матеріалів і теорія споруд*. 2019. № 103. С. 208–218. <https://doi.org/10.32347/2410-2547.2019.103.208-218>.
18. Miroshnikov V. Yu., Protsenko V. S. Determining the stress state of a layer on a rigid base weakened by several longitudinal cylindrical cavities. *Journal of Advanced Research in Technical Science*. 2019. Iss. 17. P. 11–21. <https://doi.org/10.26160/2474-5901-2019-17-11-21>.
19. Miroshnikov V. Yu., Medvedeva A. V., & Oleshkevich S. V. Determination of the stress state of the layer with a cylindrical elastic inclusion. *Materials Science Forum*. 2019. Vol. 968. P. 413–420. <https://doi.org/10.4028/www.scientific.net/MSF.968.413>.
20. Miroshnikov V. Yu., Savin O. B., Hrebennikov M. M., Pohrebniak O.A. Analysis of the stress state of a layer with two cylindrical elastic inclusions and mixed boundary conditions. *Journal of Mechanical Engineering – Problemy mashynobuduvannia*. 2022. Vol. 25. No. 2. P. 22–29. <https://doi.org/10.15407/pmach2022.02.022>.
21. Гребенніков М. М., Миронов К. В. Аналіз напруженого стану шару з поздовжньою порожниною та заданими невласно мішаними граничними умовами. *Наука, теорія і практика: тези доповідей XXIX Міжнародної науково-практичної конференції*. Японія, Токіо, 2021. С. 536–540.
22. Miroshnikov V. Rotation of the layer with the cylindrical pipe around the rigid cylinder. In: *Advances in Mechanical and Power Engineering. CAMPE 2021. Lecture Notes in Mechanical Engineering*. Cham: Springer. P. 314–322. [https://doi.org/10.1007/978-3-031-18487-1\\_32](https://doi.org/10.1007/978-3-031-18487-1_32).